Journal of Inorganic and Organometallic Polymers and Materials (2022) 32:1370–1380
https://doi.org/10.1007/s10904-021-02200-0

Removal of Ce(IV) and Nd(III) from Acidic Solution Using Polyacrylonitrile-Encapsulated Lithium Titanium Vanadate as an Efficient Adsorbent

M. Khalil[1] · H. A. Madbouly[1] · E. M. Abu Elgoud[1] · I. M. Ali[1]

Received: 29 October 2021 / Accepted: 13 December 2021 / Published online: 20 January 2022
© The Author(s), under exclusive licence to Springer Science+Business Media, LLC, part of Springer Nature 2021

Abstract
In the present study, polyacrylonitrile was grafted onto lithium titanium vanadate (LTV) to form a lithium titanium vanadate-encapsulated polyacrylonitrile (PAN/LTV). PAN/LTV composite was analyzed by FTIR, SEM, XRD, and TG–DTA. The effects of contact time, adsorbent dose, ion concentrations, solution pH and reaction temperature were evaluated in batch tests. At pH 2.5, the adsorbent showed 62.6 and 20.02% efficiency for Ce(IV) and Nd(III). For Ce(IV) and Nd(III), the PAN/LTV adsorption capacities were 7.5 mg/g and 1.2 mg/g, respectively. A Langmuir adsorption model fit well the adsorption data for Ce(IV) and Nd(III). As a result of the thermodynamic parameters, it appears the adsorption process was spontaneous and endothermic, and at the interface between the solid and solution, randomness increased. Citric acid at pH 3 successfully desorbs the adsorbed Ce(IV) and Nd(III) ions from PAN/LTV. Additionally, PAN/LTV exhibited a higher separation factor (SF) in the separation of Ce(IV)/Nd(III) ions with respect to pH and phase ratio.

Keywords Polyacrylonitrile · Lithium · Titanium · Vanadate · Adsorption · Cerium · Neodymium

1 Introduction

The disposal of radioactive waste has become a barrier to progress in the use of reactors and nuclear plants for various uses in the production of electricity and the applications of radioactive materials in research and medicine [1–3]. As it produces high quantities of radioactive waste, whether such as these low-level radioactive wastes resulting from research and medicine applications, medium-level wastes result from treatment of reactor water and high-level wastes produced from spent fuel from the reactors [4, 5]. The use of nuclear reactors always results in radiological accidents around the world, such as what happened in Japan in 2011 [6]. As a result of the earthquake and tsunami that occurred in Japan, water up to 15 meters high inundated the Fukushima nuclear power plant [7]. This led to the leakage of high-level radionuclides, such as ^{90}Sr, ^{110m}Ag, ^{129m}Te, ^{134}Cs, and ^{137}Cs, $^{142,\ 144}$Ce and ^{150}Nd and other radioactive substances [8, 9]. This radiation leak has caused global concern and fear, as this radiation, if not disposed of, will transfer to water and from there to soil and end up in plants to become part of animals and humans [10, 11].

Cerium and neodymium occurs in the minerals monazite and bastnasite and is a product of nuclear fission products of uranium, plutonium, and thorium [12–14]. The long half-lives of cerium-142 as 5×10^{16} years and of neodymium-150 as 7.9×10^{18} years were emitting release both beta particles and gamma rays, but their toxicities are primarily caused by the beta particles [15, 16]. These radioisotopes produce toxicities in the tissues of the animals and humans [17]. Therefore, it is necessary to prevent migration of these radionuclides to the biosphere and develop progressive retention techniques [18, 19].

Also there are different application in industry of cerium and neodymium as in electric motors and generators, as well as in spindle magnets for computer hard drives and wind turbines [13, 20]. So, the extract of cerium and neodymium from different sources, as in monazite, bastnasite and in nuclear fission products waste, is very important and urgent.

The interest in the elements cerium and neodymium led to the use of different methods of researchers, whether

✉ M. Khalil
magdykhalil7@yahoo.com

[1] Hot Laboratories and Waste Management Center, Egyptian Atomic Energy Authority (EAEA), P. No. 13759, Cairo, Egypt

to remove them from radioactive waste or separate them from their ores. Many methods are concerned with separating different metal ions due to their importance or danger. These methods include ion exchange, adsorption, precipitation, flotation, membrane, biosensor and solvent extraction [21–28]. The fact that the separation technology is inexpensive, environmentally friendly and easy to use is one of the important advantages of the separation method, which is evident by using the adsorption technology [27, 29]. The inorganic materials are among the most used in adsorption for their thermal and radiation stability, but they suffer from the smoothness and suspension of granules in the liquid media, which leads to the blockage of the column used in the separation, which causes difficulty in using them in the separating column [30, 31]. Also, the use of organic materials as adsorbents that have high advantages of their high capacity and their stability in acidic media, but they suffer from their lack of thermal stability [32, 33]. To obtain the characteristics of both the organic and inorganic materials, the organic materials were incorporated into the inorganic matrix [34–38].

Among the many benefits of titanium-based compounds, including their large surface area, strong ion exchange capacity, and lack of secondary pollution, is their remarkable sorption ability as a green technology for environmental pollutants such as MXenes and chitosan [28, 39].

Lithium titanium vanadate (LTV) has a higher adsorption efficiency than titanium vanadate (TV) [40]. However, LTV has many disadvantages in terms of its practical application, including easy aggregation, difficult separation, and recovery. To enhance the adsorption performance and structure, it is necessary to add additives during the synthesis process. Therefore, for easy isolation and reuse of the adsorbent in a, aqueous media, LTV has been immobilized on solid supports such as polyacrylonitrile (PAN). This process endows the inorganic phase more mechanical as well as handle facilities. In addition to the many physical and chemical advantages, PAN provides a low cost, high porosity, and high adhesion strength, which makes it a competitive alternative to other organic adsorbents [38, 41–43]. These various advantages of PAN make it an organic material that greatly improves the properties of inorganic adsorbents [44–46].

In this work, the in-situ oxidative polymerization of a good mechanical property homopolymer (PAN) on amorphous LTV was employed. A novel PAN/LTV adsorbent was tested for separation of Ce(IV) and Nd(III) ions. In this way the objective of this study is were to investigate performance of the adsorbent and to establish optimal conditions for recovery and separation of Ce(IV) and Nd(III) from aqueous solution. The sorption data were interpreted using Langmuir and Freundlich isotherms. Various thermodynamic parameters, including the mean free energy of sorption, were determined. The effect of pH and V/m ratio for probability separation of Ce(III) from Nd(III) was investigated. The recovery of Ce(IV) and Nd(III) from PAN/LTV was also investigated.

2 Experimental

2.1 Materials and Methods

All reagents and chemicals utilized in this work were of analytical grade purity and purchased from Sigma-Aldrich.

2.2 Preparation of PAN/LTV

First, lithium titanium vanadate (LTV) was prepared using a single step precipitation process through the dropwise addition of equal volumes of 0.25 M LiCl (MW = 42.39, purity ≥ 99.99%), 0.5 M $TiCl_4$ (dissolved in 2 M HCl), and 0.5 M $NaVO_3$ at pH 11 with constant stirring. Ammonia solution was used as precipitating agent.

Second, polyacrylonitrile homopolymer (PAN) was prepared by mixing equal volumes of 10% acrylonitrile and 0.1 M potassium persulfate ($K_2S_2O_8$) solutions and heating to 70 °C with continuous stirring by a magnetic stirrer. Polyacrylonitrile gel was obtained by keeping the solution at 70 °C for half an hour.

Modification of the physico-chemical properties of LTV was conducted by using a binding of polyacrylonitrile (PAN) with the inorganic precipitate for the preparation of larger size particles with higher granular strength to form the new composite adsorbent (PAN/LTV).

In details, the prepared PAN gel was added to LTV (in 20/80 W/W) and mixed thoroughly with constant stirring as shown in Fig. 1. The resultant deep green color gel PAN/LTV was kept for 24 h at room temperature (25 ± 2 °C) for digestion. The supernatant liquid was decanted, and the gel was rewashed with bidistilled water to remove fine adherent particles and was filtered using a centrifuge (4000 rpm), and dried at 60 ± 1 °C. The dried composite was cracked in DMW and converted to H^+-form by treating with 0.1 M HNO_3 for 24 h with occasional shaking intermittently replacing the supernatant liquid with fresh acid. The excess acid was removed from little washing with DMW, dried at 60 ± 1 °C till a constant weight and sieved to obtain particles with the size range 0.4–0.6 mm. Finally, the PAN/LTV was stored at room temperature for further use.

2.3 Preparation the Aqueous Solutions

Cerium (IV) (1.0 g/L) stock solution was prepared by dissolving a known amount of cerium ammonium nitrate ($Ce(NH_4)_2(NO_3)_6$) in deionized water. Stock solution of Nd(III) (1.0 g/L) was prepared by dissolving a known

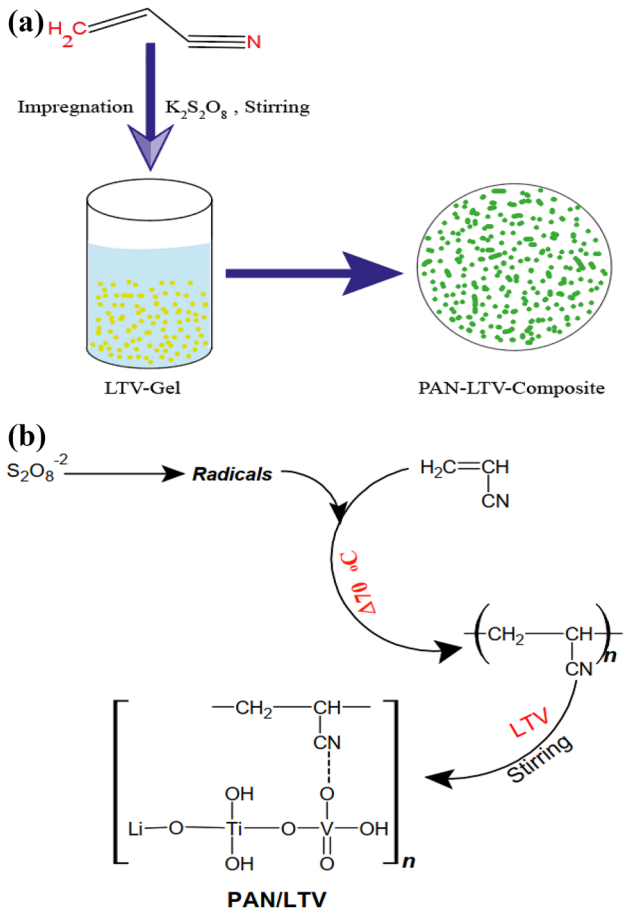

Fig. 1 **a** Preparation and **b** schematic representation of PAN/LTV composite

amount of the metal oxide in minimum concentrated nitric acid and evaporated to near dryness and then made up to the mark with double distilled water. Required concentrations of test solutions were prepared by proper dilution of the stock solutions.

2.4 Determination of Metal Ions Concentrations

The individual concentration of Ce(IV) or Nd(III) in the aqueous solution was spectrophotometrically determined using the Arsenazo–III method (Marczenko 1986), by measuring the maximum absorbance at 650 nm with a Shimadzu double beam recording UV–Vis spectrophotometer model 160 A, Japan.

2.5 Sorption Procedures

Sorption behavior of the PAN/LTV composite for removal of Ce(IV) or Nd(III) has been studied at different conditions such as, pH, contact time, ion concentrations and reaction temperatures. The effect of V/m ratio was carried at different V/m ratios ranged from 0.033 to 0.1 at initial concentration of 100 mg/L for each of Ce(IV) and Nd(III) at pH 2.5, equilibrium time 30 min and temperature degree 25 °C. The influence of pH solution ranged from 1 to 3 on the adsorption of Ce(IV) and Nd(III) was investigated at initial ion concentration 100 mg/L, equilibrium time 30 min and 25 °C. The effect of agitation was monitored for different period of times varying from 10 to 120 min at initial concentration of 100 mg/L of each of Ce(IV) and Nd(III), pH 2.5 and reaction temperature 25 °C. The effect of initial metal concentrations were carried at different concentrations ranged from 50 to 250 mg/g for Ce(IV) and 50–200 mg/g for Nd(III) at pH 2.5, equilibrium time 30 min, $V/m = 0.1$ L/g and 25 °C. The effect of temperatures in the range of 25–55 °C on the adsorption efficiency of Ce(IV) and Nd(III) was also investigated. For each experimental, the mixture was shaken for sufficient periods of time in a thermostatic shaker water bath at a speed of 200 rpm. Ce(IV) and Nd(III) concentrations in the samples was measured after the reaction period was completed using a UV–vis spectrophotometer at 650 nm in adsorption experiments. As a result of the obtained data, the optimum conditions for the removal of the studied ions were recommended. The percentage adsorption Eq. (1), distribution coefficient of (K_d) Eq. (2), and the quantity of ion adsorbed on PAN/LTV at that time, t by q_t (mg/g), Eq. (3) was calculated from the equations as follows:

$$Sorption, \% = \frac{(C_0 - C_e)}{C_e} x100 \tag{1}$$

$$K_d, ml/g = \frac{(C_0 - C_e)}{C_e} x \frac{V}{m} \tag{2}$$

$$q_e, mg/g = \frac{(C_0 - C_e)xV}{m} \tag{3}$$

where C_0 and C_e are the initial concentration and equilibrium concentration of ion solution (mg/L) respectively; V the suspension volume; and m is the amount of adsorbent used (g). in the present work

2.6 Separation Factor and Desorption Studies

The separation factor may be considered as the relative tendency of two ions to be adsorbed in an exchanger from solutions of equal concentration. It is used as a measure of possibility of chromatographic separation and is also expressed as the ratio of the distribution coefficients of the elements to be separated as:

$$\text{Separation factor } (\alpha AB) = \frac{K_d(A)}{K_d(B)} \tag{4}$$

where; K_d (A) and K_d (B) are the distribution coefficients for the two competing species Ce(IV) and Nd(III) in the ion-exchange system.

The recovery of Ce(IV) and Nd(III) from loaded on PAN/LTV adsorbent was also carried out using different reagents of various concentration ranges such as HNO_3, HCl, H_2SO_4, citric acid and NaOH.

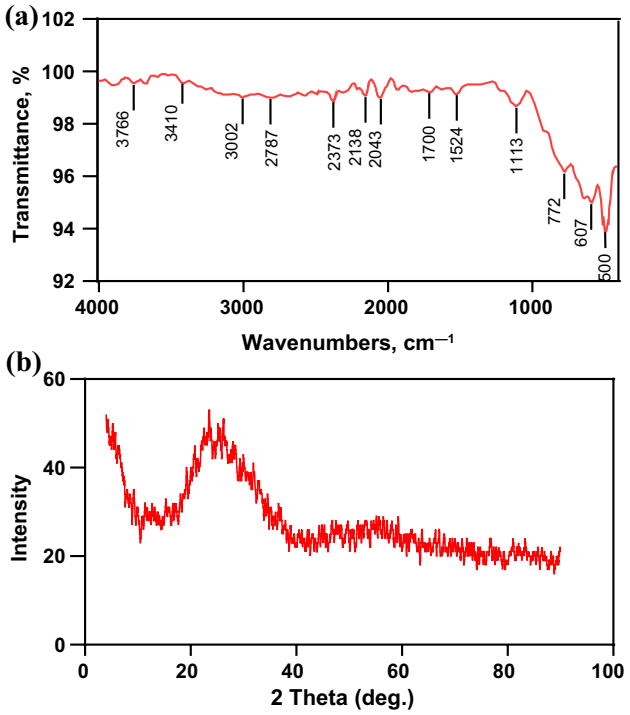

Fig. 2 **a** FTIR and **b** XRD spectrum of PAN/LTV composite

3 Results and Discussions

3.1 Characterization of PAN/LTV

The dispersion of lithium titanium vanadate (LTV) in PAN has been successfully used for the removal and/or separation of Ce(IV) and Nd(III) in aqueous solution. The FTIR spectrum (Fig. 2 a) of the PAN/LTV has the following characteristic bands. The band observed at ~ 3766 cm^{-1} represents O–H stretching vibration. The band observed at ~ 3410 cm^{-1} represents the N–H stretching vibration. The bands at 3002 cm^{-1} and 2787 cm^{-1} reflect the C-H stretching vibrations in the PAN chains, respectively. The band at 2373 cm^{-1} corresponded to the stretching vibration of nitrile (C≡N) groups. The bands at 2138 cm^{-1} and 2043 cm^{-1} were related to ν(C–CN). The band at 1700 cm^{-1} is related to C = C stretching vibration. The band at 1524 cm^{-1} is related to bending vibration of N–H. The band at 1113 cm^{-1} was related to N–H bending. The appearance of broad band at 770–480 cm^{-1} was due to the C = C bending and metal coordination.

In Fig. 2b, powder XRD was used to examine the crystallinity of PAN/LTV composite particles. As a result, the prepared composite has a singlet diffraction peak at 2θ of 23.5. This confirms that semicrystalline phase materials may be suitable for sorption operations.

The PAN/LTV was characterized through scanning electron microscopy (SEM) in order to analyze the surface morphology and compare it to the PAN/LTV loaded with Ce(IV) and Nd(III) as in Fig. 3 (a-c). SEM images of PAN/LTV with and without Ce(IV) or Nd(III) have almost the same shape.

The thermal decomposition of PAN/LTV (Fig. 4) up to 350 °C with a maxima endothermic peak at 156.5 °C for PAN/LTV was around 9.6% due to the loss of water or solvent molecules on the composite [47, 48]. In the second

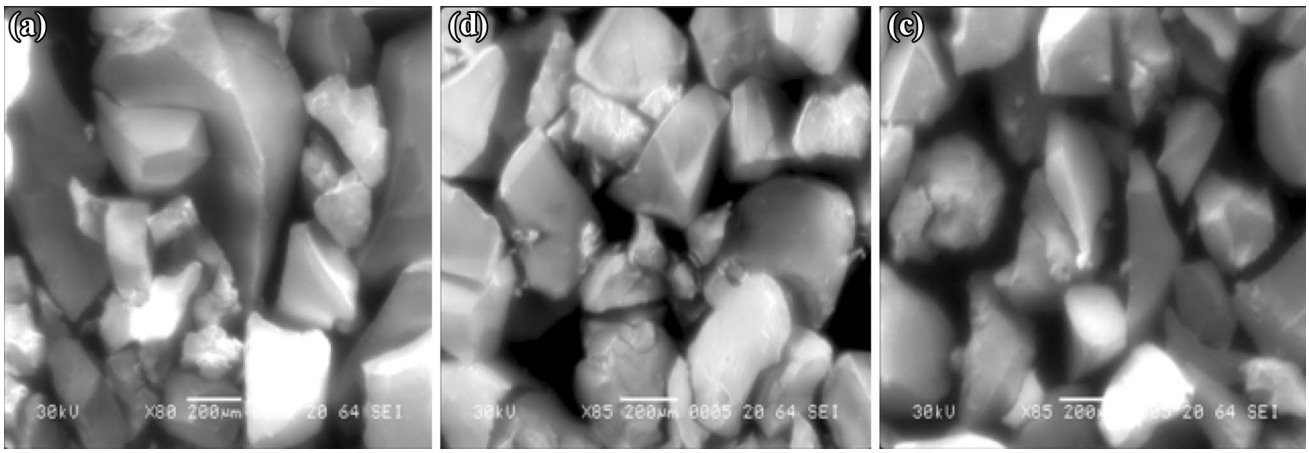

Fig. 3 SEM images of **a** PAN/LTV **b** PAN/LTV/Ce and **c** PAN/LTV/Nd

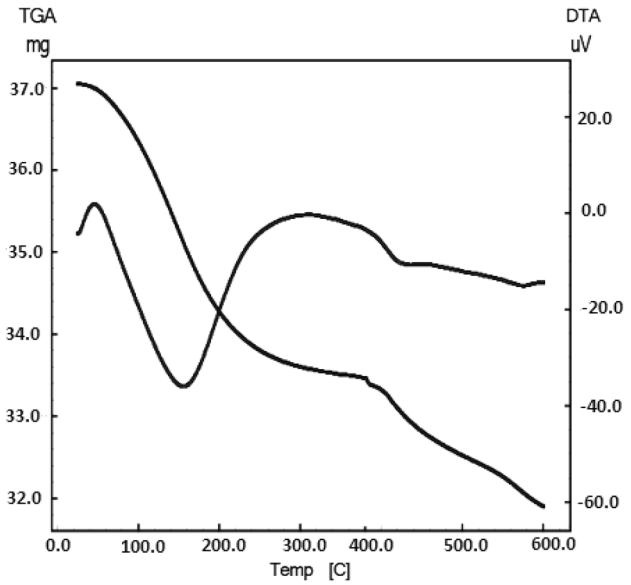

Fig. 4 DT-TGA thermogram of PAN/LTV composite

event, starting at 400 °C, there was an endothermic peak at 421 °C followed by a weight loss of 4.1% up to 600 °C. This change may be due to the loss of organic content [49]. The small and later change may be due to transform to the oxide form of the composite. According to the TGA curve, the large weight decomposition of the PAN occurred between 450 and 680 °C was ≈ 75% [49]. PAN/LTV showed a total water loss of 13.70% up to 600 °C, demonstrating its high thermal stability due to the incorporation of LTV into PAN.

X-ray fluorescence spectrometry was used to determine the percent of Ti(IV), V(VI) and Li in the PAN/LTV. Table 1 shows the weight percent composition of the PAN/LTV and the expected empirical formula is $(TiO_2)_{1.75}$ (V_2O_5) $(Li_2O)_{0.25}$ $(H_2O)_{3.70}$/PAN.

3.2 Factors Affecting the Sorption of Ce(IV) and Nd(III) on PAN/LTV

3.2.1 Effect of V/m Ratio

The effect of changing V/m (L/g) ratio on the sorption of Ce(IV) and Nd(III) on PAN/LTV adsorbent at pH 2.5 was investigated in the V/m range of 0.033– 0.10 L/g. Figure 5. shows the results obtained, as the V/m ratio decreases, the sorption increases. With a decrease in V/m from 0.1 to 0.033 L/g, the sorption efficiency (%) increased from 58.26 to 84.61%, while about 9.56% to 31.47%, in Ce(IV) and Nd(III), respectively. Even though the sorption efficiency increases with decrease in V/m ratio, the experimental work on separation feasibilities between the investigated metal species was performed at V/m of 0.1 L/g.

Table 1 Chemical composition of PAN/LTV composite

Composition of PAN/LTV	Element, %
PAN	10
TiO_2	33.1
V_2O_5	42.2
Li_2O	2.25
H_2O	12.45

3.2.2 Effect of Solution pH

In adsorption of metal ions, pH is a critical parameter as it determines the surface charge and the site of adsorption and ionization of the adsorbates [50]. Where, pH depends on the metal species in aqueous solution as well as the surface properties of the adsorbent based on its functional group. The sorption of Ce(IV) and Nd(III) from aqueous solutions was affected by pH between 1.0 and 3.0, as shown in Fig. 6. The results showed that Ce(IV) and Nd(III) sorption efficiency increased as pH increased from 1.0 to 2.5. After increasing pH to 3.0, the sorption percent slightly increased for Nd(III), however, for Ce(IV), the sorption percent decreased due to cerium precipitation. Due to the competitive adsorption between metal ions and H^+ in strong acid conditions, adsorbents for metal ions at lower pH 1 exhibit lower absorbency [51]. However, as pH increased, the concentration of H^+ ions decreased, resulting in reduced protonation and more vacant sites available for metal ion adsorption. For Ce(IV) or Nd(III) at pH 2.5, the maximum adsorption uptake values were 62.6 and 20.02%, respectively. Therefore, pH 2.5 was suggested as an optimum pH value for other experiments of sorption of the studied metal ions from aqueous solutions.

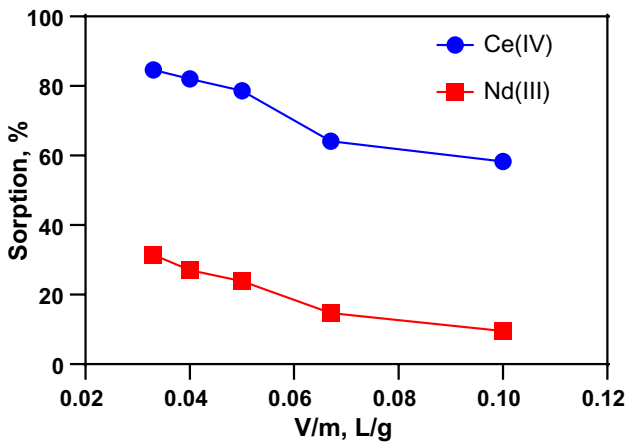

Fig. 5 Effect of V/m ratio on the sorption efficiency of Ce(IV) and Nd(III) on PAN/LTV at 100 mg/L, pH 2.5, shaking time 30.0 min and 25 °C

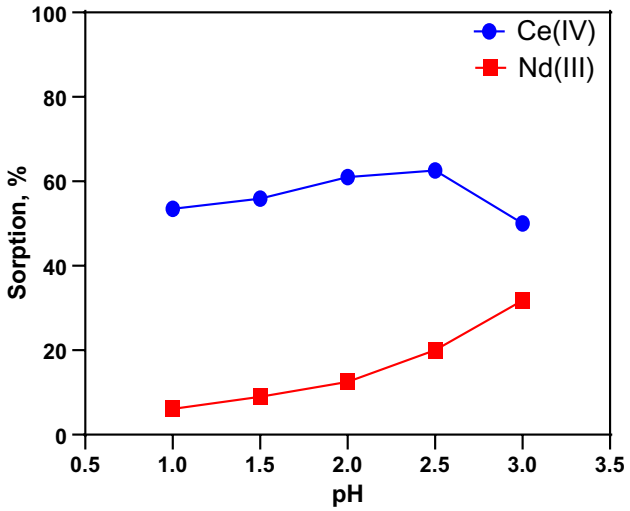

Fig. 6 Effect of pH on the sorption of Ce(IV) and Nd(III) on PAN/LTV at 100 mg/L, *V/m* = 0.1 L/g and 25 °C

3.2.3 Effect of Contact Time

As shown in Fig. 7, the effect of shaking time on the sorption of Ce(IV) and Nd(III) on PAN/LTV adsorbent from aqueous solution was tested in the range of 10.0–120.0 minutes. In Fig. 7, the sorption percentage of Ce(IV) and Nd(III) increases with the shaking time up to 30.0 minutes, then remains constant with further shaking time increases. The sorption of Ce(IV) and Nd(III) onto PAN/LTV is a fast process. Only 30 min is sufficient for Ce(IV) and Nd(III) adsorption to reach equilibrium. The rapid adsorption of Ce(IV) and Nd(III) ions is attributed to the abundance of surface sites on the PAN/LTV [52].

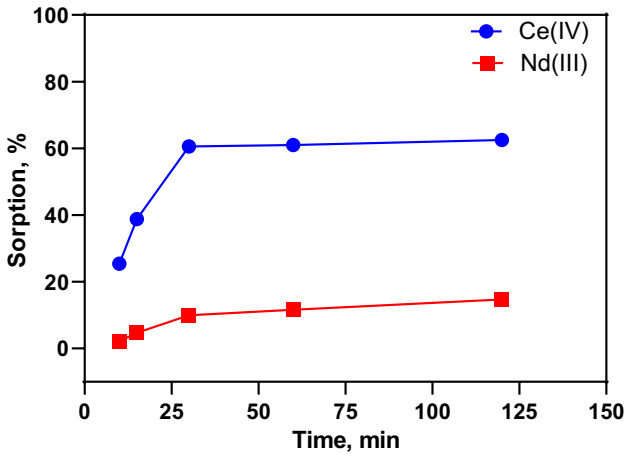

Fig. 7 Effect of shaking time on the sorption of Ce(IV) and Nd(III) on PAN/LTV at 100 mg/L, pH 2.5, *V/m* = 0.1 L/g and 25 °C

3.2.4 Effect of Initial Metal Concentration

The effect of the initial metal ion concentration on the sorption efficiency of Ce(IV) and Nd(III) in the range 50.0 – 250.0 for Ce(IV) and 50.0 – 200.0 for Nd(III) mg/L was studied by using PAN/LTV adsorbent from aqueous solution, whereas the other factors, such as equilibration time, pH, and adsorbent quantity, remained constant. The results showed that metal concentration decreased sorption efficiency, as shown in Fig. 8. With an increase in the initial concentration, the sorption percent for Ce(IV) and Nd(III) decreased from 77.19% to 26.16% and from 24.1% to 4.99%, respectively [33].

3.2.5 Effect of Reaction Temperature

Temperature effects on the sorption of Ce(IV) and Nd(III) on PAN/LTV adsorbed from aqueous solution with pH 2.5 were studied at different temperatures in the range 15–65 °C. In Fig. 9, it can be observed that the sorption of these metal ions slightly decreases with increasing temperature. In the sorption process the thermodynamic parameters of free energy change ΔG^{o}, enthalpy change ΔH^{o}, and entropy change ΔS^{o} can be calculated as follows:

$$\Delta G^{\circ} = -RTLnK_{d} \quad (5)$$

$$\Delta G^{\circ} = \Delta H^{\circ} - T\Delta S^{\circ} \quad (6)$$

$$-RT\ Ln\ K_{d} = \Delta H^{\circ} - T\Delta S^{\circ} \quad (7)$$

$$Ln(q_{e}/C_{e}) = (\Delta S^{\circ}/R) + (-\Delta H^{\circ}/R)1/T \quad (8)$$

where $K_{d} = q_{e}/C_{e}$ (mL/g), R is the universal gas constant (8.314 J/mol K) and T is the absolute temperature (K).

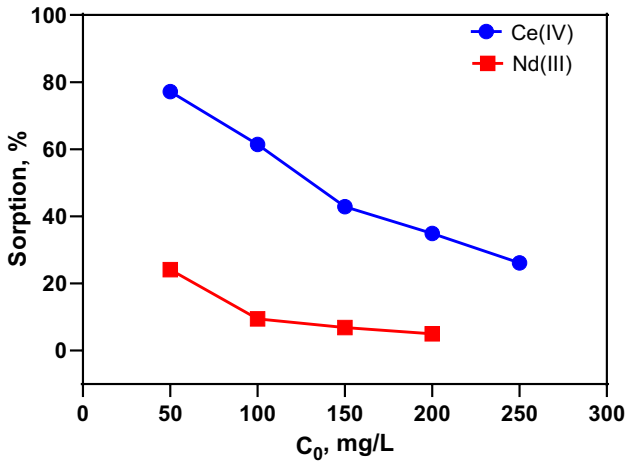

Fig. 8 Effect of the initial concentration on the sorption efficiency of Ce(IV) and Nd(III) on PAN/LTV at pH 2.5, shaking time 30.0 min and *V/m* = 0.1 L/g and 25 °C

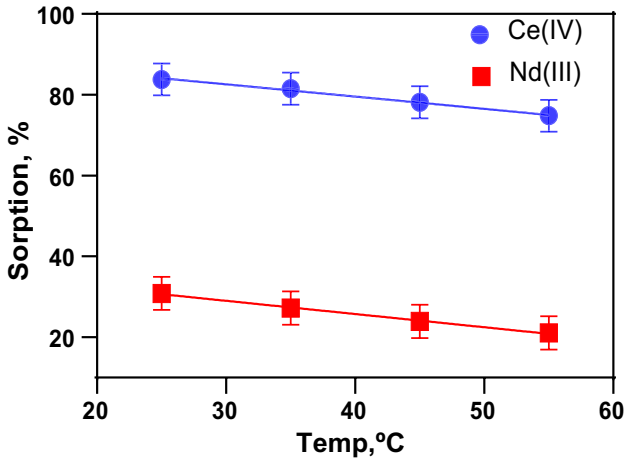

Fig. 9 Effect of temperature on the sorption efficiency of Ce(IV) and Nd(III) on PAN/LTV at 100 mg/L, pH 2.5, and shaking time 30.0 min

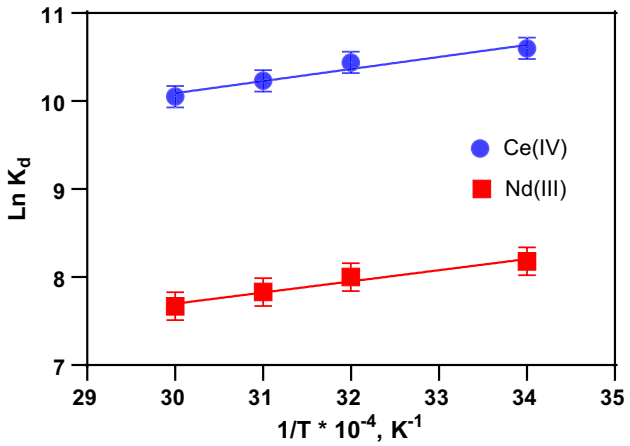

Fig. 10 Relation between Ln K_d and 1/T on the sorption efficiency of Ce(IV) and Nd(III) on PAN/LTV at 100 mg/L, pH 2.5, shaking time 30.0 min, V/m = 0.033 L/g and 25 °C

The plot of ln K_d versus 1/T would result in a straight line with a slope of (- ΔH^o/R) and intercept of (ΔS^o/R) as shown in Fig. 10. The values of ΔG^o, ΔH^o and ΔS^o are tabulated in Table 2. The ΔG^o value for Ce(IV) and Nd(III) ions was negative, indicating that the sorption processes were feasible and spontaneous. Ce(IV) sorption is more feasible than Nd(III) sorption according to the values in Table 2. The negative values of ΔH^o correspond to an exothermic sorption process, whereas the positive values of ΔS^o reflect a randomization of the system [29].

3.3 Sorption Isotherm Modeling

By testing the solution concentration for the interaction with Ce(IV) and Nd(III) ions, the PAN/LTV adsorbent was evaluated for the adsorption capacity with the large number of active sites. The experimental data was interpreted by linear Langmuir and Freundlich sorption isotherms.

Table 2 Thermodynamic parameters for the sorption of Ce(IV) and Nd(III) ions onto PAN/LTV composite

Thermodynamic parameter	Ce(IV)	Nd(III)
ΔH^o, kJ mole^{-1}	− 11.4	− 10.54
ΔG^o, kJ mole^{-1}	− 26.20	− 20.18
ΔS^o, J mole^{-1} K^{-1}	49.68	32.36

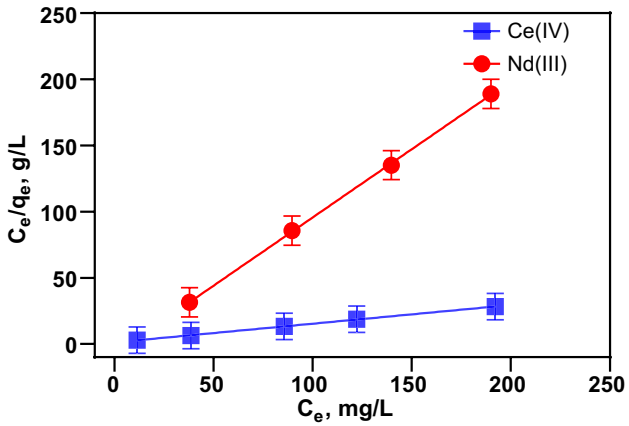

Fig. 11 Langmuir isotherm for the sorption of Ce(IV) and Nd(III) on PAN/LTV composite

3.4 Langmuir Isotherm Model

The monolayer adsorption capacity, q_o (mg/g) was calculated by the linear Langmuir equation:

$$\frac{C_e}{q_e} = \left(\frac{1}{q_0}\right)b + \left(\frac{1}{q_0}\right)C_e \tag{9}$$

Figure 11 shows the plot of C_e/q_e against C_e for Ce(IV) and Nd(III) sorption. In Table 3, the monolayer adsorption capacity q_o (mg/g) and Langmuir constant (b) of each of the metal ions were calculated from the slope and intercept of the plot. R_L can be expressed as a dimensionless constant referred to as the equilibrium parameter in the Langmuir isotherm model, which is given by the following equation:

$$R_L = \frac{1}{1 + bC_0} \tag{10}$$

Table 3 gives the Langmuir model's R_L value. In all concentrations studied, the R_L values were $1 > R_L > 0$, indicating high favorable sorption of Ce(IV) and Nd(III) on PAN/

Table 3 Langmuir and Freundlich parameters for sorption of Ce(IV) and Nd(III) ions onto PAN/LTV composite

Metal ions	q_e, exp mg/g	Langmuir parameters				Freundlich Parameters		
		q_o (mg/g)	b (ml/mg)	R_L	R^2	K_f (mg/g)	1/n	R2
Ce(IV)	7.90	7.09	0.12	0.08	0.999	2.49	0.21	0.835
Nd(III)	1.15	0.98	0.126	0.075	0.989	1.81	0.12	0.905

LTV adsorbent. The experimental sorption capacities for Ce(IV) and Nd(III) were found to be comparable to the calculated sorption capacities determined from the Langmuir model, as shown in Table 3. The maximum Langmuir adsorption capacities (q_o) for Ce(IV) and Nd(III) were 7.09 and 0.98 mg/g respectively. This number is very close to the measured values of 7.90 mg/g for Ce(IV); and 1.15 mg/g for Nd(III). Therefore, the Langmuir model is valid for explaining the sorption results, indicating that the monolayer adsorption process can explain the metal adsorption [32, 53]. The Ce(IV) was more adsorption than Nd(III) due to the difference in the oxidation state.

3.5 Freundlich Isotherm Model

This linear equation of the Freundlich isotherm model is expressed as:

$$\log q_e = \log K_f + \frac{1}{n} \log C_e \quad (11)$$

K_F is a parameter of the Freundlich equation used to measure adsorption capacity (mg/g), and 1/n measures adsorption intensity. Figure 12 shows the plot of log q_e (mg/g) versus log C_e (mg/L). For Ce(IV) and Nd(III), the K_f and 1/n were calculated using the slope and intercept of the plots, and are listed in Table 3. Among the investigated metal ions, the slope of the Freundlich isotherm is less than 1, $1 > 1/n > 0$, and equals 0.21 in case of Ce(IV) and 0.12 in case of Nd(III). There is a favorable adsorption for the different metal's ions investigated on the PAN/LTV adsorbent. As a result, this model is unable to justify the experimental capacity for different metals where the values of K_f obtained from this model are significantly lower than the experimental values, as shown in Table 3. Also, the correlation coefficient R^2 values for the Langmuir equation were 0.999 or 0.989 for Ce(IV) or Nd(III) respectively which indicated that the Langmuir isotherm better fitted the experimental data than the Freundlich model and could better explain the Ce(IV) or Nd(III) adsorption process. Thus, the Freundlich model does not fully explain the experimental results for these elements [54]. To compare the cerium and neodymium ions adsorption performance obtained in this study, Table 4 presents results in literature found using other adsorbent materials. Cerium and neodymium are weakly adsorbed compared to some research, but the possibility of separating Ce(IV) from Nd(III) makes PAN/LTV composites a promising material in the separation of these ions.

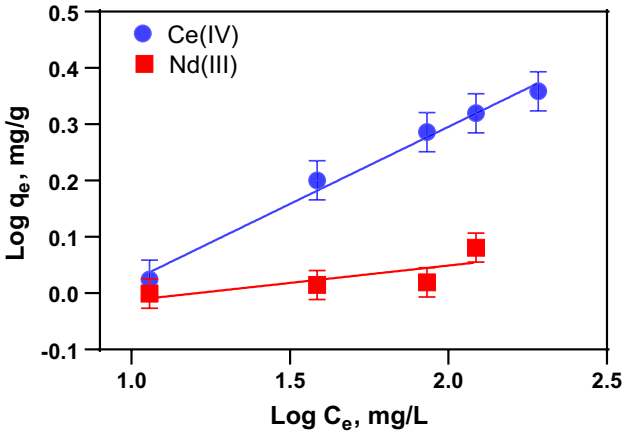

Fig. 12 Freundlich isotherm for the sorption of Ce(IV) and Nd(III) on PAN/LTV composite

Table 4 A comparison of the adsorption capacities for Ce(IV) and Nd(III) by PAN/LTV and other reported adsorbents

Adsorbents	Adsorption capacity (mg/g)		Reference
	Ce	Nd	
PAN/LTV	7.09	0.98	This work
Nitrolite	4.45	4.13	[55]
CYANEX 272-MNPs		4.8	[56]
Activated carbon	9. 66		[57]
dMNP-DTPA		0.353	[58]
Carbon black from recycled tires	5.04		[59]
clay minerals		1.587	[60]
Chrysotile nanotubes	0.17		[61]
Fe3O4@TiO2@P_20_4		8.66	[62]
MIL-101	11.3		[50]
Fe3O4@SiO2@polyaniline GO		8.5	[63]
Alkyl phosphinic acid resin		2.02	[64]

3.6 Separation Feasibility and Desorption Studies

Table 5 shows the calculated separation factors (SF) for Ce(IV), and Nd(III) ions at different pH values. According to

Table 5 the highest separation factors for Ce(IV) and Nd(III) are 17.83 and 12.86 at pH values of 1.0 and 1.5, respectively. In addition, we can also obtain good separation between Ce(IV), and Nd(III) at different phase ratios, as shown in Table 6. Based on Table 6, the highest separation factors between Ce(IV) and Nd(III) are 13.21, 12.33, and 11.97 at V/m ratios of 0.1, 0.04, and 0.03 L/g, respectively.

Different reagents of various concentration ranges were used to recover Ce(IV) and Nd(III) from PAN/LTV adsorbed material. The reagents included hydrochloric acid, sulfuric acid, nitric acid, ammonium carbonate, sodium hydroxide, and citric acid. The desorption experiments were carried out in an aqueous solution of hydrochloric acid and sulfuric acid, whereby it was found that the recovered amounts of Ce(IV) and Nd(III) were negligible. The low recovery of Ce(IV) and Nd(III) may be attributed to the strong binding between Ce(IV) and Nd(III) on PAN/LTV. It is clear that recovery of Nd(III) can be accomplished with 1.0 M HNO_3 in which 68.7% recovery can be achieved. The recovered amounts of Ce(IV) and Nd(III) were 20.35 and 21.78%, respectively using 1.0 M of sodium hydroxide. According to Table 7, citric acid at pH = 3.0 is the best stripper for the two metal ions, where the recovered amounts of Ce(IV) and Nd(III) were 46.41 and 21.76, respectively.

Table 6 Effect of phase ratio on the separation of Ce(IV) from Nd(III) on PAN/LTV composite

V/m, L/g	Separation factors (SF) of Ce/Nd
0.1	13.21
0.07	10.34
0.05	11.72
0.04	12.33
0.033	11.97

4 Conclusion

PAN/LTV composite was successfully prepared with incorporated lithium titanium vanadate with polyacrylonitrile. PAN/LTV was well characterized using different techniques. The optimum conditions for adsorption of Ce(IV) and Nd(III) onto PAN/LTV were achieved as pH 2.5, equilibrium time was 30 min and initial concentration was 100 mg/L and V/m ratio was 0.1 L/g. PAN/LTV adsorption capacities were 7.5 mg/g for Ce(IV) and 1.2 mg/g for Nd(III). The adsorption process was fit well with a Langmuir adsorption model. The thermodynamic results indicate that sorption is exothermic and spontaneous, and an increase in randomness in the system. Ce(IV) and Nd(III) have the highest separation factors in acidic solutions at pH 1.0 and they have a separation factor of 13.21 at a V/m ratio of 0.1 L/g. Results of stripping experiments revealed maximum stripping rates of 46.4 and 21.76% for Ce(IV) and Nd (III), respectively, at pH = 3.0 using 1.0 mol / L citric acid.

Acknowledgements The authors thank all the staff members of Nuclear Fuel Technology Department, Hot Laboratories Centre, Egyptian Atomic Energy Authority for their cooperation, and useful help offered during this work.

Declarations

Conflict of interest The authors declare that they have no known competing financial interests or personal relationships that could have appeared to influence the work reported in this paper

Table 5 Effect of pH on the separation of Ce(IV) from Nd(III) on PAN/LTV composite

pH	Separation factors (SF) of Ce/Nd
1.0	17.83
1.5	12.86
2.0	8.54
2.5	6.67

Table 7 Desorption of Ce(IV) and Nd(III) on PAN/LTV using different reagents

Stripping agent	Concentration, M	Desorption percent, %	
		Ce(IV)	Nd(III)
HNO_3	1.0	5.4	68.7
HCl	1.0	0	0
H_2SO_4	1.0	0	1.15
Citric acid	1.0 (pH = 1.0)	40.71	4.69
	1.0 (pH = 3.0)	46.41	21.76
NaOH	1.0	20.35	21.78
Ammonium carbonate	1.0	0	ppt

References

1. D.S. Wisnubroto, H. Zamroni, R. Sumarbagiono, G. Nurliati, Nucl. Eng. Technol. (2020). https://doi.org/10.32479/ijeep.9765
2. S. Kashurnikov, V. Prasolov, V. Gorbanyov, R. Rogulin, Int. J. Energy Econ. Policy **10**, 131 (2020)
3. D. Deng, L. Zhang, M. Dong, R.E. Samuel, A. Ofori-Boadu, M. Lamssali, Water Environ. Res. **92**, 1818 (2020)
4. A. Taş, A.Y. Özer, FABAD J. Pharm. Sci. **45**, 91 (2020)
5. M. Lersow, P. Waggitt, *Dispos. All Forms Radioact. Waste Residues* (Springer, Cham, 2020), pp. 235–315
6. S. Omama, N. Komoribayashi, Y. Inoue, T. Mase, K. Ogasawara, Y. Ishibashi, M. Ohsawa, T. Onoda, K. Itai, K. Tanno, Cerebrovasc. Dis. Extra **10**, 105 (2020)
7. K. Goto, T. Ishizawa, Y. Ebina, F. Imamura, S. Sato, K. Udo, Earth-Science Rev. **212**, 103417 (2020)
8. T. Watanabe, N. Tsuchiya, Y. Oura, M. Ebihara, C. Inoue, N. Hirano, R. Yamada, S. Yamasaki, A. Okamoto, F.W. Nara, Geochem. J. **46**, 279 (2012)
9. Y. Okumura, K. Kaneko, H. Ota, H. Nagasaka, M. Hara, Pollut. Bull. **157**, 111235 (2020)
10. K. Hirose, J. Environ. Radioact. **111**, 13 (2012)
11. Y. Oura, M. Ebihara, H. Tsuruta, T. Nakajima, T. Ohara, M. Ishimoto, H. Sawahata, Y. Katsumura, W. Nitta, J. Nucl. Radiochem. Sci. (2015). https://doi.org/10.14494/jnrs.15.2_1
12. R. Doucelance, N. Bellot, M. Boyet, T. Hammouda, C. Bosq, Earth Planet. Sci. Lett. **407**, 175 (2014)
13. L. Omodara, S. Pitkäaho, E.-M. Turpeinen, P. Saavalainen, K. Oravisjärvi, R.L. Keiski, J. Clean. Prod. **236**, 117573 (2019)
14. T. Ohno, T. Hirata, Anal. Sci. **29**, 47 (2013)
15. N.N. Wanna, A. Dobney, K. Van Hoecke, M. Vasile, F. Vanhaecke, Talanta **221**, 121592 (2021)
16. M.F. Horan, R.W. Carlson, R.J. Walker, M. Jackson, M. Garçon, M. Norman, Earth Planet. Sci. Lett. **484**, 184 (2018)
17. S. Madhav, A. Ahamad, A.K. Singh, J. Kushawaha, J.S. Chauhan, S. Sharma, P. Singh, *Sensors Water Pollut. Monit. Role Mater* (., Cham, 2020), pp. 43–62
18. L.T. Townsend, K. Morris, J.R. Lloyd, *Microbiol Nucl Waste Dispos* (Elsevier, Amsterdam, 2020), pp. 245–265
19. M. Lersow, P. Waggitt, *Dispos. All Forms Radioact. Waste Residues* (Springer, Cham, 2020), pp. 317–395
20. S. Verma, R. Gupta, K.K. Bamzai, Mater. Res. Bull. **81**, 71 (2016)
21. I. Rodríguez-Ruiz, S. Teychené, Y. Vitry, B. Biscans, S. Charton, Chem. Eng. Sci. **183**, 20 (2018)
22. M. Gras, N. Papaiconomou, E. Chainet, F. Tedjar, I. Billard, Sep. Purif. Technol. **178**, 169 (2017)
23. A. Ferdowsi, H. Yoozbashizadeh, Trans. Nonferrous Met. Soc. China **27**, 420 (2017)
24. E. Jorjani, A.H. Bagherieh, S. Mesroghli, S.C. Chelgani, J. Univ. Sci. Technol. Beijing Miner. Metall. Mater. (2008). https://doi.org/10.1007/978-3-030-32910-5_1
25. E. Karal, M.A. Kucuker, B. Demirel, N.K. Copty, K. Kuchta, J. Clean. Prod. **288**, 125087 (2020)
26. E. Allahkarami, B. Rezai, J. Environ. Chem. Eng. **9**, 104956 (2021)
27. I.M. Ali, E.S. Zakaria, M. Khalil, A. El-tantawy, F.A. El-Saied, J. Inorg. Organomet. Polym. Mater. **30**, 1537 (2020)
28. S. Ramanavicius, A. Ramanavicius, Int. J. Mol. Sci. **21**, 9224 (2020)
29. E.S. Zakaria, I. Mali, M. Khalil, T.Y. Mohamed, A. EL-Tantawy, Bull. Mater. Sci. **39**, 1709 (2016)
30. M. Khalil, Y.F. El-Aryan, I.M. Ali, J. Inorg. Organomet. Polym. Mater. **26**, 359 (2016)
31. I.M. El-Naggar, E.S. Zakaria, I.M. Ali, M. Khalil, M.F. El-Shahat, J. Environ. Radioact. **112**, 108 (2012)
32. M. Khalil, Y.F. El-Aryan, E.M. El Afifi, Part. Sci. Technol. **36**, 618 (2018)
33. M. Khalil, T.Y. Mohamed, A. El-tantawy, J. Inorg. Organomet. Polym. Mater. **27**, 757 (2017)
34. H. Zhang, J. Ma, F. Wang, Y. Chu, L. Yang, M. Xia, Int. J. Biol. Macromol. **149**, 1161 (2020)
35. P. Yin, Q. Xu, R. Qu, G. Zhao, Y. Sun, J. Hazard. Mater. **173**, 710 (2010)
36. J. Xu, S. Virolainen, W. Zhang, J. Kuva, T. Sainio, R. Koivula, Chem. Eng. J. **351**, 832 (2018)
37. D.L. Ramasamy, V. Puhakka, B. Doshi, S. Iftekhar, M. Sillanpää, Chem. Eng. J. **365**, 291 (2019)
38. R. Zhang, Y. Ma, W. Lan, D.E. Sameen, S. Ahmed, J. Dai, W. Qin, S. Li, Y. Liu, Ultrason. Sonochem. **70**, 105343 (2021)
39. Z. Xu, Y. Yu, L. Yan, W. Yan, C. Jing, J. Environ. Sci. **112**, 202 (2022)
40. I.M. Ali, M.A. Gomaa, I.M. El Naggar, J.A. Omar, M.F. El-Shahat, Desalin. Water Treat. **57**, 14552 (2016)
41. I. Toumi, H. Djelad, F. Chouli, and A. Benyoucef, J. Inorg. Organomet. Polym. Mater. 1 (2021).
42. N.M. Mahmoodi, Z. Mokhtari-Shourijeh, S. Langari, A. Naeimi, B. Hayati, M. Jalili, K. Seifpanahi-Shabani, J. Mol. Struct. **1227**, 129418 (2021)
43. Y. Liu, X. Dong, K. Bao, Z. Deng, M.A. Hossen, J. Dai, W. Qin, K. Lee, J. Environ. Chem. Eng. **9**, 106801 (2021)
44. X. Chen, D. Chen, N. Li, Q. Xu, H. Li, J. He, J. Lu, A.C.S. Appl, Mater. Interfaces **12**, 39227 (2020)
45. Z.-Q. Feng, X. Yuan, T. Wang, Chem. Eng. J. **392**, 123730 (2020)
46. J. Bai, J. Chu, X. Yin, J. Wang, W. Tian, Q. Huang, Z. Jia, X. Wu, H. Guo, Z. Qin, Chem. Eng. J. **391**, 123553 (2020)
47. O. Kazak, A. Tor, I. Akin, G. Arslan, J. Environ. Chem. Eng. **3**, 1654 (2015)
48. S. Almuhamed, M. Bonne, N. Khenoussi, J. Brendle, L. Schacher, B. Lebeau, D.C. Adolphe, J. Ind. Eng. Chem. **35**, 146 (2016)
49. R.E. Neisiany, S.N. Khorasani, J.K.Y. Lee, S. Ramakrishna, RSC Adv. **6**, 70056 (2016)
50. Y.-R. Lee, K. Yu, S. Ravi, W.-S. Ahn, A.C.S. Appl, Mater. Interfaces **10**, 23918 (2018)
51. W. Feng, W. Wenbo, Z. Yongfeng, W. Aiqin, J. Rare Earths **35**, 697 (2017)
52. M. Khalil, M.M. Shehata, O. Ghazy, S.A. Waly, Z.I. Ali, Radiat. Phys. Chem. **190**, 109811 (2022)
53. E.S. Zakaria, I.M. Ali, M. Khalil, A. El-Tantawy, F.A. El-Saied, J. Radioanal. Nucl. Chem. **330**, 1271–1280 (2021)
54. I.M. Ali, M. Khalil, H.A. Madbouly, A.M. Soliman, Int. J. Environ. Anal. Chem. (2021). https://doi.org/10.1080/03067319.2021.1912332
55. G. Wójcik, Materials (Basel). **13**, 2256 (2020)
56. L. Molina, J. Gaete, I. Alfaro, V. Ide, F. Valenzuela, J. Parada, C. Basualto, J. Mol. Liq. **275**, 178 (2019)
57. M.R. Mahmoud, G.E.S. El-deen, M.A. Soliman, Ann. Nucl. Energy **72**, 134 (2014)
58. H. Zhang, R.G. Mcdowell, L.R. Martin, Y. Qiang, A.C.S. Appl, Mater. Interfaces **8**, 9523 (2016)
59. Y.R. Smith, D. Bhattacharyya, T. Willhard, M. Misra, Chem. Eng. J. **296**, 102 (2016)
60. X. Yanfei, L. Huang, L. Zhiqi, F. Zongyu, W. Liangshi, J. Rare Earths **34**, 543 (2016)
61. L. Cheng, S. Yu, C. Zha, Y. Yao, X. Pan, Chem. Eng. J. **213**, 22 (2012)
62. P. Yan, M. He, B. Chen, B. Hu, Spectrochim. Acta Part B At. Spectrosc. **136**, 73 (2017)
63. S. Su, B. Chen, M. He, B. Hu, Z. Xiao, Talanta **119**, 458 (2014)
64. Q. Fu, L. Yang, Q. Wang, Talanta **72**, 1248 (2007)

Publisher's Note Springer Nature remains neutral with regard to jurisdictional claims in published maps and institutional affiliations.